

# Anomaly Detection in Sonar Images Based on Wavelet Domain Noncausal AR-ARCH Random Field Modeling

Saman Mousazadeh

Faculty of Electrical Engineering  
Technion - Israel Institute of Technology

Israel Cohen

Faculty of Electrical Engineering  
Technion - Israel Institute of Technology

**Abstract**—In this paper we introduce a novel anomaly detection method in sonar images based on noncausal autoregressive-autoregressive conditional heteroscedasticity (AR-ARCH) model. The background of the sonar image in the wavelet domain is modeled by a noncausal AR-ARCH model. Matched subspace detector (MFD) is used for detecting the anomaly in the image. The proposed method is computationally efficient and is robust to the orientation variation of the image, compared to competing method.

**Index Terms**—Noncausality, AR-ARCH, Anomaly detection, Sonar images.

## I. INTRODUCTION

Image anomaly detection is the process of extracting a small number of clustered pixels, which are different from the background. The type of image and the characteristics of anomalies are application dependent. Among the applications one can name detection of targets in images, detection of defects in silicon wafers, detection of mine features in side-scan sonar and detection of tumors in medical imaging. Target detection in radar and sonar imagery is a challenging problem due to the large variability in background clutter and in object appearance. The detection of sea-mines, for example, involves addressing the varying shape of the ocean surface and its vegetation [1]. In most cases, lethal targets must be detected with nearly 100% reliability. False detections may not be disastrous but might slow down the demining process.

Anomaly detection algorithms generally consist of some or all of the following stages: selection of an appropriate feature space, selection of a statistical model for the selected feature space and selection of a detection algorithm.

A proper selection of a feature space, which allows distinction of anomalies from the clutter, is an important part of an anomaly detection algorithm. Feature space selection methods can be classified into two major groups: Image pixel feature space and transform feature space. In *image pixel feature space*, the feature space is created based on the image pixels themselves. Kazantsev et al. [2] introduced a feature space based on two circular concentric windows  $W_1$  and  $W_2$  with radii  $R_1$  and  $R_2$ , respectively,  $R_1 < R_2$ . A similar approach is taken by Schweizer and Moura [3]. In their approach two concentric rectangles serve as the moving window. For further

discussion on this kind of feature space selection see [2] and [3]. In *transform feature space*, the feature space is created based on the transformed image. There exist two common transforms which are mainly used for anomaly detection: Karhunen-Loeve transform (KLT) and discrete wavelet transform (DWT). The KLT is used to transform an  $n$  dimensional vector space into an  $m$  dimensional vector space, where  $m < n$ , such that the mean-square magnitude of the error resulting from representing the  $n$  dimensional vector using only  $m$  dimensions is minimized. The KLT is also used to remove correlation between features. DWT is recently used in variety of applications in image signal processing. Among them, the most important one is image compression and coding [4]. The theory of two dimensional DWT is well developed and can be found in classic textbooks, (see [4]).

Once the feature space is chosen, one must find an appropriate statistical model to describe the natural clutter in the selected feature space domain. Popular models for modeling the natural clutter are gaussian or extensions of gaussian, selected because of their mathematical tractability. Ashton [5] performed subpixel anomaly detection in multispectral infrared imagery using gaussian distribution for clutter. Stein et al. [6] used a gaussian mixture model (GMM) for modeling hyperspectral imagery. Other extensions such as linear mixing model (LMM) and Gauss Markov random field (GMRF) are used by several authors for modeling the clutter. See [7] for a good review of multi-resolution Markov models for signal and image processing. Recently, Noiboar and Cohen [8] used *causal* GARCH model for anomaly detection in sonar images. The causality assumption incorporated into the GARCH model in [8], is unnatural for images. Developing a non-causal statistical model characterized by a heavy tailed distribution and innovation clustering leads to an improvement in clutter modeling by reducing the dependency on image orientation. As a result, such a model, may reduce the false alarm rate for a given detection rate.

By anomaly detection we mean classifying a region of an image as anomaly or background with the assumption of low-probability anomalies. There are several anomaly detector among them one can name single hypothesis test (SHT) [9], matched filter detector (MFD) and its adaptive version

[10], matched subspace detector (MSD) [11] and its adaptive version [12].

In this paper, we present a new statistical model to describe the natural clutter in DWT domain. This model generalizes the method presented in [8] by using a noncausal ARCH instead of GARCH model. The rest of the paper is organized as follows. In section 2, we introduce the noncausal two-dimensional AR-GARCH model and our anomaly detector which is based on two dimensional AR-GARCH modeling of the clutter. In section 3, we evaluate the performance of the proposed algorithms using simulations.

## II. NONCAUSAL AR-ARCH MODELING OF THE IMAGES IN WAVELET DOMAIN AND ANOMALY DETECTION

In this section we introduce a noncausal AR-ARCH model for images in the wavelet domain and anomaly detection procedure. This model is to some extent similar to the model used in [8] with a major difference. The model used in [8] is a causal model whereas our proposed model is noncausal. Let  $z(t_1, t_2)$  be the original image. Using two dimensional wavelet transform introduced in [8], we get a set of  $2L + 1$  images where  $L$  is the depth of the wavelet transform. We utilize an undecimated wavelet transform. The undecimated wavelet transform has the property of translation invariance, which is important in the context of anomaly detection. Let  $y_\ell(t_1, t_2)$ ;  $1 \leq \ell \leq 2L + 1$  be the  $\ell$ -th image in the wavelet domain. We assume that the background image is a noncausal AR-ARCH process defined as follows

$$y_\ell(t_1, t_2) = \sum_{i=-r}^r \sum_{j=0}^s b_{i,j}^\ell y_\ell(t_1 - i, t_2 - j) + \sum_{i=-r}^r \sum_{j=0}^s b_{i,j}^\ell y_\ell(t_1 + i, t_2 + j) + x_\ell(t_1, t_2) \quad (1)$$

$$x_\ell(t_1, t_2) = \sigma_\ell(t_1, t_2) \varepsilon_\ell(t_1, t_2) \\ \sigma_\ell^2(t_1, t_2) = c_0^\ell + \sum_{i=-p}^p \sum_{j=0}^q a_{i,j}^\ell x_\ell^2(t_1 - i, t_2 - j) + \sum_{i=-p}^p \sum_{j=0}^q a_{i,j}^\ell x_\ell^2(t_1 + i, t_2 + j) \quad (2)$$

where  $b_{i,j}^\ell$  are parameters of the AR part,  $\forall i \leq 0$ ,  $b_{i,0}^\ell = 0$ ,  $r$  and  $s$  are the order of AR model in horizontal and vertical directions,  $c_0$  and  $a_{i,j}$  are the parameters of the ARCH part,  $\forall i \leq 0$ ,  $a_{i,0} = 0$ ,  $p$  and  $q$  are the order of the ARCH model in horizontal and vertical directions and  $\varepsilon_\ell(t_1, t_2)$  are zero mean independent identically distributed (IID) random variables with identity covariance matrix. We have defined our two dimensional noncausal AR-ARCH model based on the definition of two dimensional noncausal AR model [13] extensively used in image signal processing.

Now we introduce a heuristic method for parameter estimation of the two dimensional noncausal AR-ARCH model. Noting that the ARCH process is white, the parameters of the

AR part can be easily estimated with the method proposed in [13]. Let this estimate of the parameters of the AR part be denoted by  $\hat{b}_{i,j}^\ell$ . Using this estimate of the parameters and (1) the residual of the AR model (i.e.,  $x_\ell(t_1, t_2)$ ) can be easily estimated as follows

$$\hat{x}_\ell(t_1, t_2) = y_\ell(t_1, t_2) - \sum_{i=-p}^r \sum_{j=0}^s \hat{b}_{i,j}^\ell y_\ell(t_1 - i, t_2 - j) - \sum_{i=-p}^r \sum_{j=0}^s \hat{b}_{i,j}^\ell y_\ell(t_1 + i, t_2 + j). \quad (3)$$

Using this estimate of the residuals, the parameters of the ARCH part can be estimated using the modified two stage least squares (MTSLS) method. This method is a generalization of TSLS method [14] to the noncausal case. Substituting this estimate of the parameters and estimate of the residuals (i.e.,  $\hat{x}_\ell(t_1, t_2)$ ) in (2), the estimate of the conditional variance is obtained as follows

$$\hat{\sigma}_\ell^2(t_1, t_2) = \hat{c}_0^\ell + \sum_{i=-p}^p \sum_{j=0}^q \hat{a}_{i,j}^\ell \hat{x}_\ell^2(t_1 - i, t_2 - j) + \sum_{i=-p}^p \sum_{j=0}^q \hat{a}_{i,j}^\ell \hat{x}_\ell^2(t_1 + i, t_2 + j) \quad (4)$$

where  $\hat{c}_0$  and  $\hat{a}_{i,j}^\ell$  are the estimates of the parameters obtained by MTSLS method.

Using this estimate of the conditional variance, the anomaly detector is obtained as follows. For each pixel in each layer  $y^\ell(t_1, t_2)$  we create a column vector  $\hat{\mathbf{x}}^\ell(t_1, t_2)$  by row stacking an image chip of size  $L_1^\ell \times L_2^\ell$  centered around pixel  $(t_1, t_2)$  in the  $\ell$ -th layer. Assume that there exists no interference and let  $\psi^\ell(t_1, t_2)$  be a vector locating the anomaly within its subspace  $\langle H_\ell \rangle = \text{span}\{H_\ell\}$ . We define two hypotheses,  $H_0$  and  $H_1$ , which respectively represent absence and presence of an anomaly as follows:

$$H_0 : \hat{\mathbf{x}}^\ell(t_1, t_2) = \sigma_\ell(t_1, t_2) \varepsilon_\ell(t_1, t_2) \quad (5)$$

$$H_1 : \hat{\mathbf{x}}^\ell(t_1, t_2) = H^\ell \psi^\ell(t_1, t_2) + \sigma_\ell(t_1, t_2) \varepsilon_\ell(t_1, t_2) \quad (6)$$

where

$$\sigma_\ell^2(t_1, t_2) = c_0^\ell + \sum_{i=-p}^p \sum_{j=0}^q a_{i,j}^\ell x_\ell^2(t_1 - i, t_2 - j) + \sum_{i=-p}^p \sum_{j=0}^q a_{i,j}^\ell x_\ell^2(t_1 + i, t_2 + j). \quad (7)$$

Under the two hypotheses the sample conditional distribution of  $\hat{\mathbf{x}}^\ell(t_1, t_2)$  is gaussian with identical covariance matrices with different means, i.e.

$$H_0 : \hat{\mathbf{x}}^\ell(t_1, t_2) \sim \mathcal{N}(\mathbf{0}, \mathbf{\Sigma}_{t_1, t_2}^\ell) \quad (8)$$

$$H_1 : \hat{\mathbf{x}}^\ell(t_1, t_2) \sim \mathcal{N}(H^\ell \psi^\ell(t_1, t_2), \mathbf{\Sigma}_{t_1, t_2}^\ell) \quad (9)$$

where  $\mathbf{\Sigma}_{t_1, t_2}^\ell$  is a diagonal matrix whose diagonal is a vector obtained by row stacking of a chip of  $\sigma_\ell^2(t_1, t_2)$  with size

$L_1^\ell \times L_2^\ell$  centered around pixel  $(t_1, t_2)$  in the  $\ell$ -th layer. The log-likelihood ratio can be computed as follows [11]

$$L_{t_1, t_2}^\ell = \left( (\Sigma_{t_1, t_2}^\ell)^{-\frac{1}{2}} \hat{\mathbf{x}}^\ell(t_1, t_2) \right)^T P_H^\ell \left( (\Sigma_{t_1, t_2}^\ell)^{-\frac{1}{2}} \hat{\mathbf{x}}^\ell(t_1, t_2) \right) \quad (10)$$

where

$$P_H^\ell = H^\ell \left( (H^\ell)^T H^\ell \right)^{-1} (H^\ell)^T. \quad (11)$$

Since the true value of the conditional variance  $(\sigma_{t_1, t_2}^\ell)$  is not available, by the generalized likelihood ratio test, it can be replaced by its estimate  $(\hat{\sigma}_{t_1, t_2}^\ell)$  which is given by (4). Our final detector is given by comparing the generalized likelihood ratio with a predefined threshold, i.e.,

$$L_{t_1, t_2}^{GLR} = \sum_{\ell=1}^{2L+1} \Gamma_\ell$$

$$\Gamma_\ell = \left( (\hat{\Sigma}_{t_1, t_2}^\ell)^{-\frac{1}{2}} \hat{\mathbf{x}}^\ell(t_1, t_2) \right)^T P_H \left( (\hat{\Sigma}_{t_1, t_2}^\ell)^{-\frac{1}{2}} \hat{\mathbf{x}}^\ell(t_1, t_2) \right)$$

$$\begin{matrix} H_1 \\ \Gamma_\ell \geq \eta \\ H_0 \end{matrix} \quad (12)$$

where  $\eta$  is the threshold level and  $\hat{\Sigma}_{t_1, t_2}^\ell$  is a diagonal matrix whose diagonal is a vector obtained by row stacking of a chip of  $\hat{\sigma}_{t_1, t_2}^\ell$  with size  $L_1^\ell \times L_2^\ell$  centered around pixel  $(t_1, t_2)$  in the  $\ell$ -th layer. The anomaly subspace for each layer  $(H^\ell)$  is estimated from a database by exactly the same approach utilized in [8]. The algorithm is summarized in Table 1.

TABLE I  
ANOMALY DETECTION ALGORITHM USING NONCAUSAL AR-ARCH  
MODEL

- (1) Transform the image to wavelet domain.
- (2) Find the anomaly subspace  $H^\ell$  for each layer.
- (3) For each layer estimate the AR parameters and the residuals (i.e.  $\hat{\mathbf{x}}^\ell(t_1, t_2)$ ) using (3).
- (4) For each layer estimate the ARCH parameters and the conditional variance (i.e.  $\hat{\sigma}^\ell(t_1, t_2)$ ) using (4).
- (5) Find the generalized likelihood ratio using (12).
- (6) Compare the generalized likelihood ratio to a threshold.

### III. SIMULATION RESULTS

In this section we evaluate the performance of our anomaly detection using simulations. We use real side-scan sonar images. The side-scan sonar images presented in these simulations are taken from the Sonar-5 database collected by the Naval Surface Warfare Center Coastal System Station (Panama City, FL). The images are 8-bit gray scale. An elongated sea mine is characterized by a bright line (the highlight or echo), corresponding to the scattering response of the mine to the acoustic insonification, and a shadow behind it, corresponding to the blocking of sonar waves by the mine.

The result for a specific image with two different orientations is depicted in Fig 1. In this simulation we used AR-ARCH model with the following orders :  $p = 1, q = 1, r = 3, s = 3$ . The size of the original signal is  $528 \times 512$  and both

$L_1^\ell$  and  $L_2^\ell$  are set to 16. The depth of the wavelet transform is equal to 4 and we used Harr wavelet transform. Other simulations show that the selection another mother wavelet does not affect the overall performance of the detector. In Fig 1 each row consists of the original picture (left), the result of the proposed detection algorithm (middle) and the result of the detection algorithm presented in [8] (right). From this figure it is apparent that the orientation of the image dose not affect the performance of the proposed method while the performance of the method presented in [8] depends on the orientation. It is worth mentioning that the computational load of the proposed method is much lower than the method presented in [8] so it can be used in real time applications.

### IV. CONCLUSION

We have presented an anomaly detection algorithm based on AR-ARCH modeling of the background. The detection algorithm is Matched Subspace Detector and the clutter model is noncausal AR-ARCH model. This model is an extension of the model used in [8] for anomaly detection. The advantage of the proposed over causal GARCH one is its low computational load and its invariability to the orientation of the image. Simulation results demonstrate the improved performance of the proposed method.

### REFERENCES

- [1] G. Dobeck and J. Hyland, "Sea mine detection and classification using side-looking sonars," in *Proc. SPIE Annual Int. Symp. Aerospace/Defense Sensing, Simulation and Control*, vol. 2496, 1995.
- [2] I. G. Kazantsev, I. Lemahieu, G. I. Salov, and R. Denys, "Statistical detection of defects in radiographic images in nondestructive testing," *Signal Processing*, vol. 82, pp. 791–801, 2002.
- [3] S. M. Schweizer and J. M. F. Moura., "Hyperspectral imagery: Clutter adaptation in anomaly detection." *IEEE Trans. Information Theory*, vol. 46, pp. 1855–1871, 2002.
- [4] D. F. Walnut, *An Introduction to Wavelet Analysis*. Birkhäuser Boston, 2004.
- [5] E. A. Ashton, "Detection of subpixel anomalies in multispectral infrared imagery using an adaptive bayesian classifier," *IEEE Trans. Geoscience and Remote Sensing*, vol. 36, pp. 506–517, March 1998.
- [6] D. W. J. Stein, L. E. H. S. G. Beaven, E. M. Winter, A. P. Schaum, and A. D. Stocker, "Anomaly detection from hyperspectral imagery," *IEEE Signal Processing Magazine*, vol. 19, pp. 58–69, January 2002.
- [7] A. S. Willsky, "Multiresolution markov models for signal and image processing," *Proc. IEEE*, vol. 90, pp. 1396–1458, August 2002.
- [8] A. Noiboar and I. Cohen, "Anomaly detection based on wavelet domain garch random field modeling," *IEEE Trans. Geoscience and Remote Sensing*, vol. 45, pp. 1361–1373, May 2007.
- [9] K. Fukunaga, *Introduction to statistical pattern recognition (2nd ed.)*. Academic Press Professional, Inc., 1990.
- [10] D. Manolakis and G. Shaw, "Detection algorithms for hyperspectral imaging applications," *IEEE Signal Processing Magazine*, vol. 19, pp. 29–43, January 2002.
- [11] L. L. Scharf and B. Friedlander, "Matched subspace detectors," *IEEE Transactions on Signal Processing*, vol. 42, pp. 2146–2157, August 1994.
- [12] S. Kraut, L. L. Scharf, and L. T. McWhorter, "Adaptive subspace detectors," *IEEE Trans. Signal Processing*, vol. 49, pp. 1–16, January 2001.
- [13] P. Y. Zhao and D. R. Yu, "An unbiased and computationally efficient LS estimation method for identifying parameters of 2-d noncausal SAR models," *IEEE Trans. Signal Processing*, vol. 41, pp. 849–857, Feb. 1993.

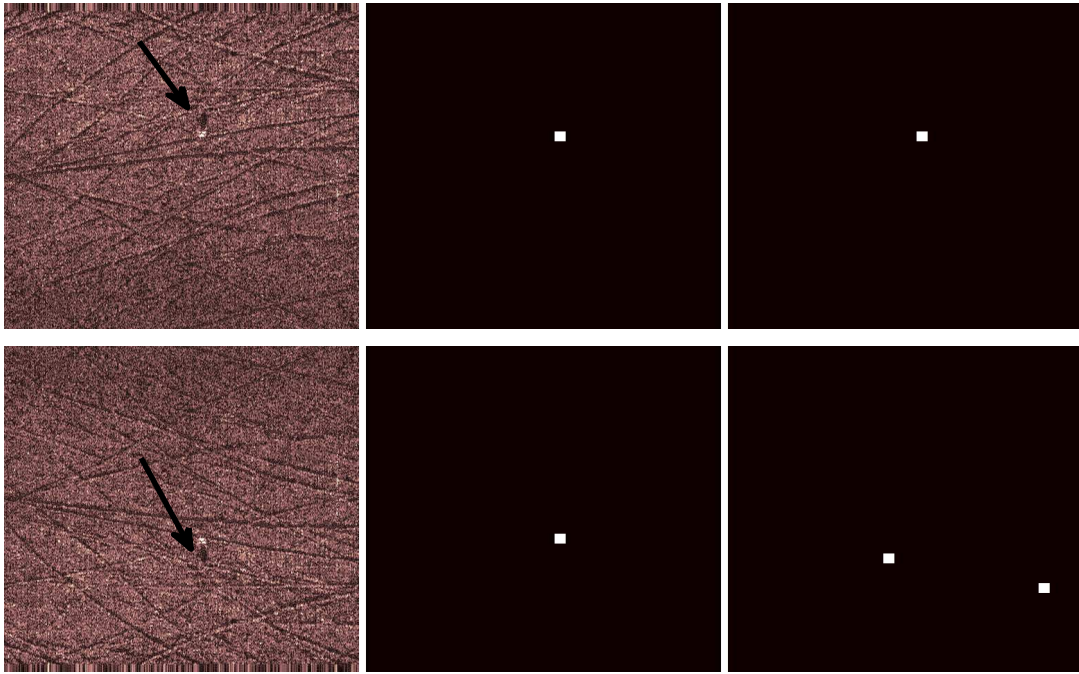


Fig. 1. Side scan sonar image with hand marked target (left), the output of the noncausal AR-ARCH based detector (middle) and the output of the GARCH based detector presented in [8] (right).

- [14] S. Mousazadeh and M. Karimi, "Estimating multivariate ARCH parameters by two-stage least-squares method," *Signal Processing*, vol. 89, pp. 921–932, May 2009.